Electronic Supplementary Information (ESI) for ***Sustainable Energy & Fuels***
This journal is © The Royal Society of Chemistry 2018

In-situ C–H activation-derived polymer@TiO_2 *p-n* heterojunction for photocatalytic hydrogen evolution

Yu-Qin Xing,[a] Zhi-Rong Tan,[a] Jing-Zhao Cheng,[a] Zhao-Qi Shen,[a] Yu-Jie Zhang,[a] Long Chen[b] and Shi-Yong Liu*[a]

[a] College of Materials, Metallurgical and Chemistry, Jiangxi University of Science and Technology, Ganzhou 341000, P. R. China

[b] Department of Chemistry, Tianjin University, Tianjin 300072, P. R. China

Corresponding author:

* E-mail: chelsy@zju.edu.cn, chelsy@jxust.edu.cn (S. -Y. Liu)

Characterization

X-ray diffraction (XRD) was measured by Thermo Fisher NexsaI instrument. X-ray photoelectron spectroscopy (XPS) was measured by Thermo Fisher NexsaI instrument. Morphology of heterojunction photocatalysts was gained by scanning electron microscope (SEM, MLA650F, American) and transmission electron microscopy (TEM, FEI Tecnai G2 F20, American). Fourier transformed infrared (FTIR) spectra were performed on a FT-IR spectrometer (Bruker, ALPHA) in the range of 4000-500 cm^{-1}. UV-vis diffuse reflectance spectra were performed on UV-2600 scanning UV-vis spectrophotometer. Time-resolved fluorescence spectroscopy and photoluminescence (PL) spectra were carried out on HORIBA Instruments FL-1000 fluorescence spectrometer. Samples were degassed under vacuum at ambient temperature for 24 h. The volume of nitrogen adsorption was recorded over a relative pressure range between 0.01 and 0.99. 8 points in the relative pressure range of 0.05-0.2 were used for the calculation of the surface area according to the Brunauer-Emmet-Teller (BET) theory. Contact angle were obtained by JCY type measurement instrument (Shanghai Fang Rui Instrument Co. Ltd.).

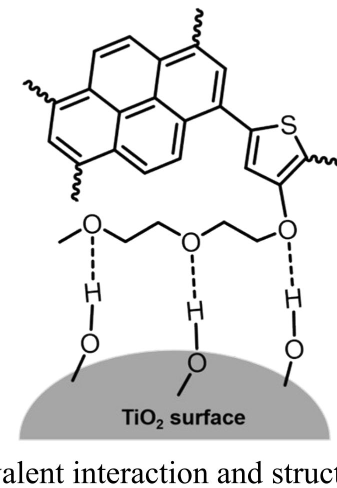

Fig. S1 Hydrogen bond non-covalent interaction and structural illustration of PyOT@TiO_2s.

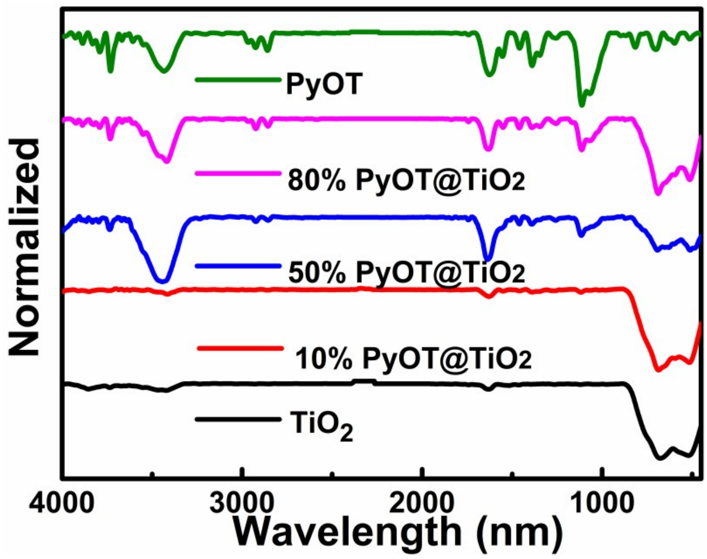

Fig. S2 FT-IR spectra of pristine TiO_2, PyOT@TiO_2s, and PyOT.

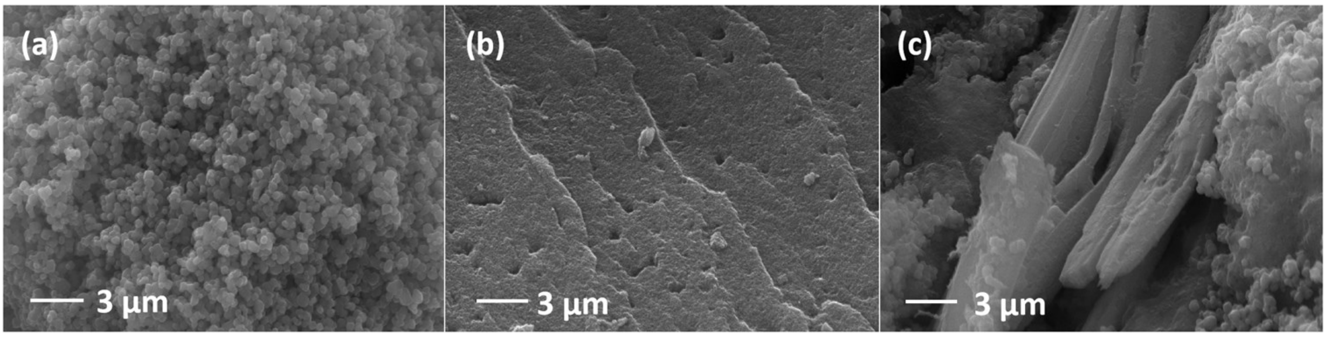

Fig. S3 SEM and TEM images of TiO_2 (a), PyOT (b), and 50% PyOT@TiO_2 (c).

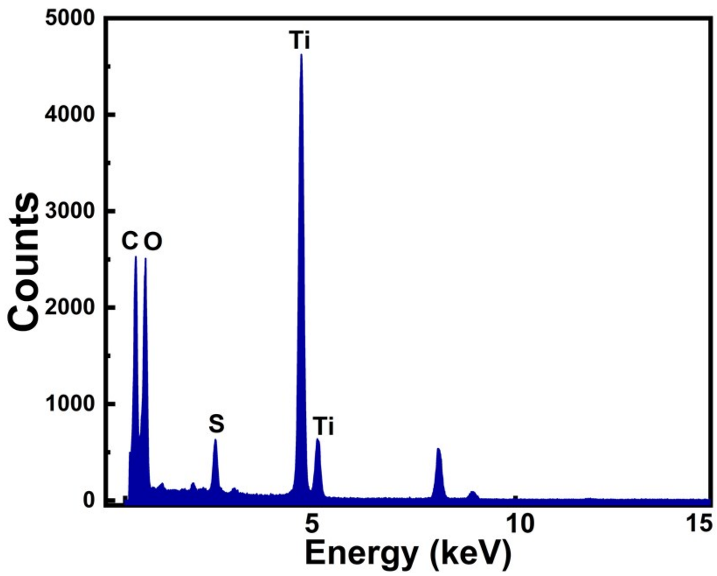

Fig. S4 EDS spectrum of 50% PyOT@TiO_2.

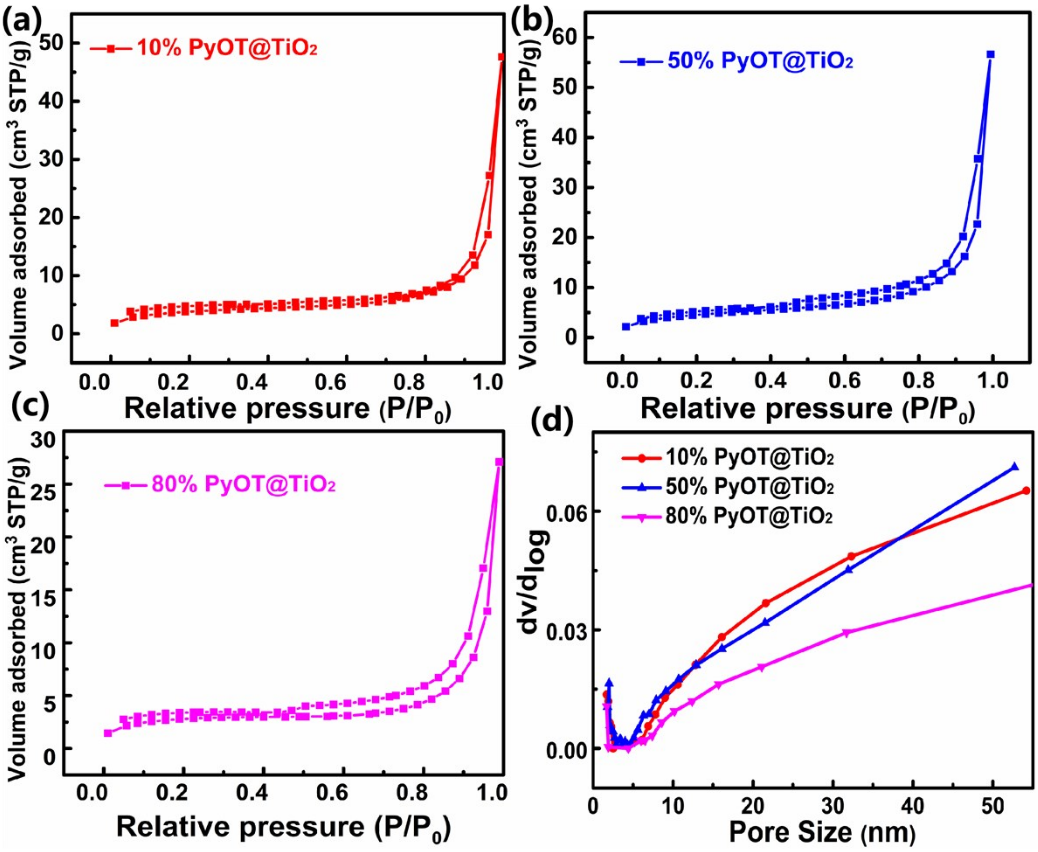

Fig. S5 (a-c) N_2 adsorption-desorption isotherms and (d) pore size distributions of 10% PyOT@TiO_2, 50% PyOT@TiO_2 and 80% PyOT@TiO_2.

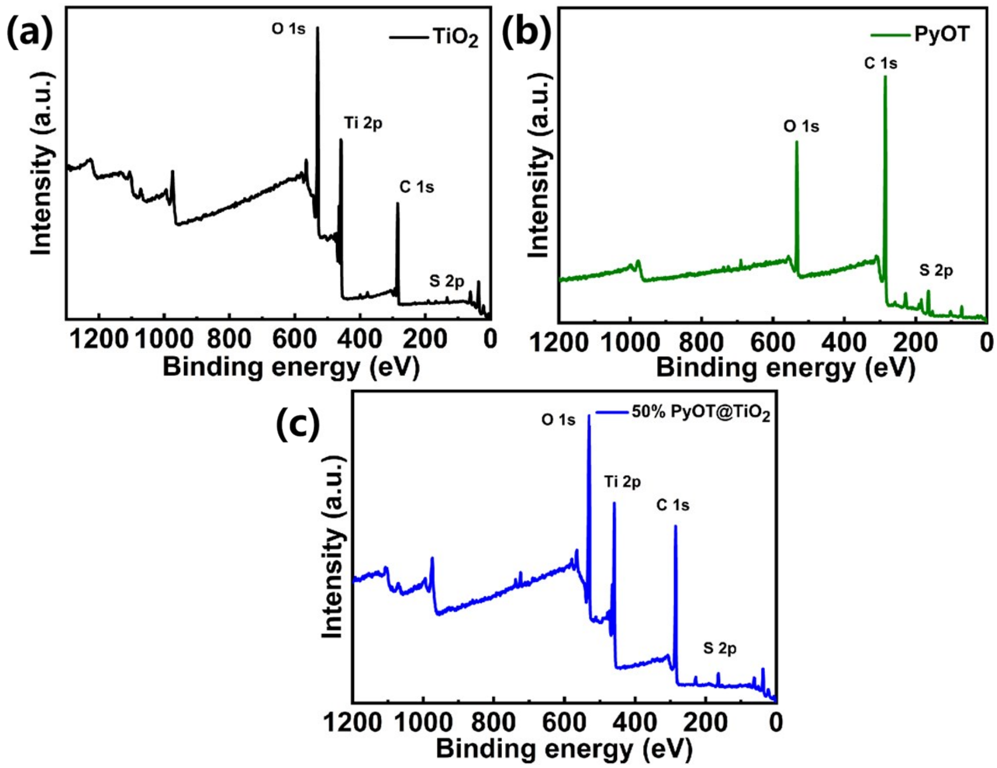

Fig. S6 XPS of TiO_2 (a) , PyOT (b), and 50% PyOT@TiO_2 (c).

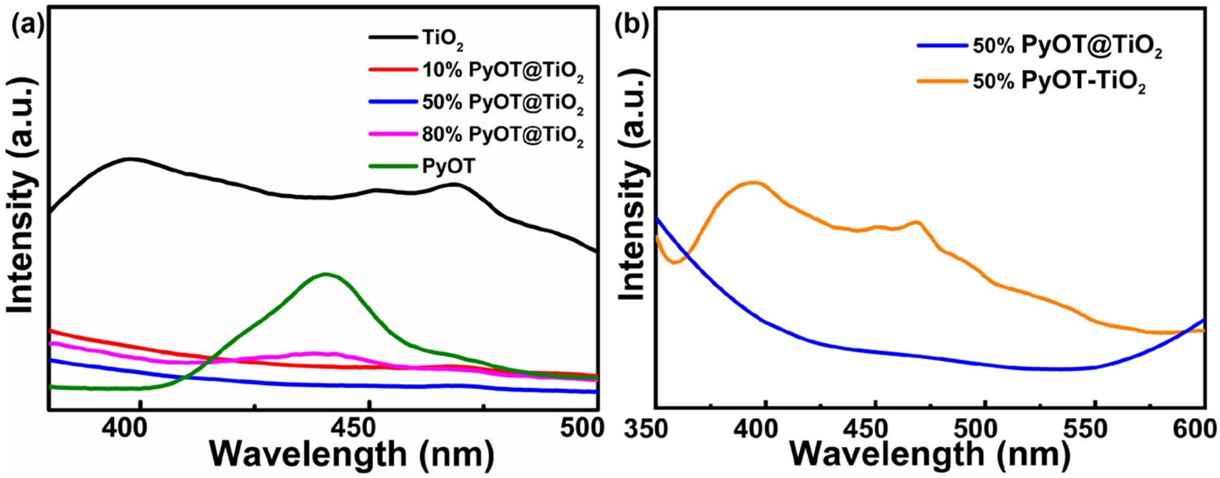

Fig. S7 Partial enlarged PL spectra of all samples (a), and PL spectra of in-situ synthesized 50% PyOT@TiO_2 and mechnically mixed 50% PyOT-TiO_2 composites (b).

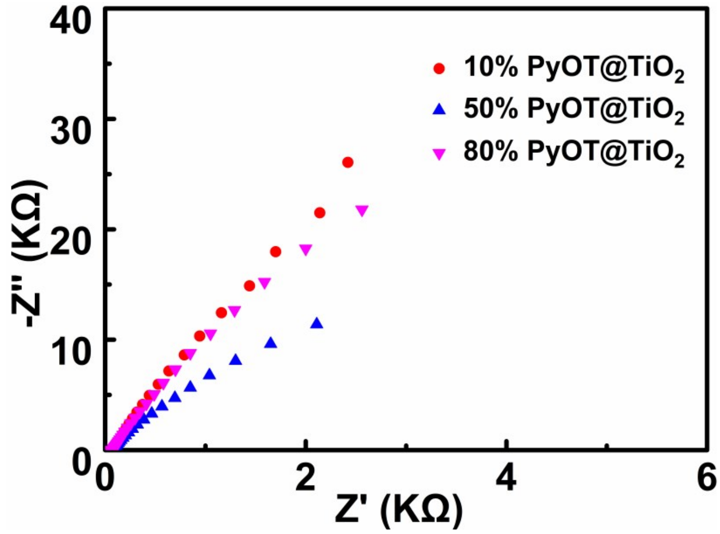

Fig. S8 EIS Nyquist plots 10% PyOT@TiO_2, 50% PyOT@TiO_2 , 80% PyOT@TiO_2 under visible light irradiation (λ ≥ 420 nm).

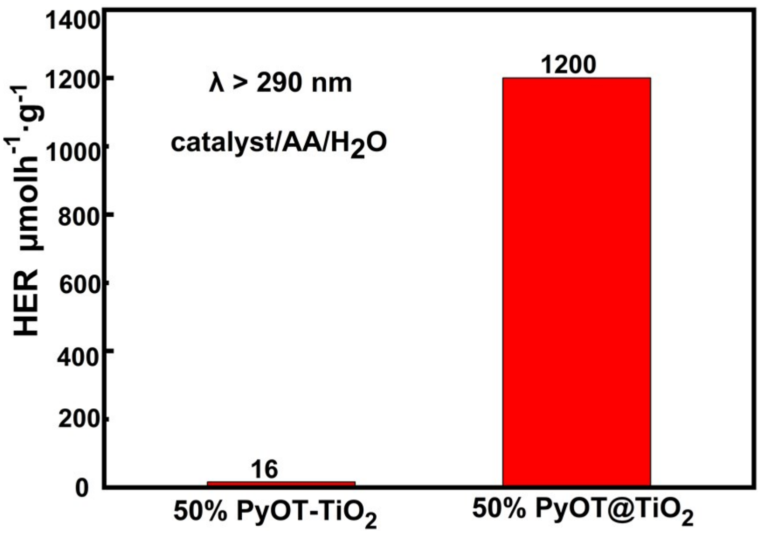

Fig. S9 HERs of 50% PyOT-TiO_2 and 50% PyOT@TiO_2.

Table S1. Comparisons of Photocatalystic HER of Various TiO_2-Based Photocatalysts.

Photocatalysts	Sacrificial agent	Light source		HER(μmol h^{-1} g^{-1})	Ref.
		Power(W)	Filter (nm)		
PyOT@TiO_2	AA	300 W Xe lamp	>420	541	This work
NiS/TiO_2 nanofibers	CH_3OH	350 W Xe lamp	>420	655	1
TiO_2/CdS	CH_3OH	350 W Xe lamp	>420	51.4	2
BE-TiO_2	TEOA	300 W Xe lamp	>420	419.2	3
TiO_2(P25)-gC_3N_4	TEOA	150 W Hg Lamp	>420	419	4
B-BT-1,4-E/TiO_2	TEOA	300 W Xe lamp	>420	220.4	5
BBT/TiO_2	TEOA	300W Xe lamp	>420	30.0	6
FeS_2–TiO_2	CH_3OH	300W Xe lamp	>420	331	7
g-C_3N_4/TiO_2	TEOA	300W Xe lamp	>420	300	8
TiO_2@g-C3N_4	CH_3OH	300W Xe lamp	>420	198	9
MoS_2/TiO_2	Na_2S+Na_2SO_3	300W Xe lamp	>420	143.32	10
FH-TiO_2	CH_3OH	300 W Hg Lamp	>420	566	11

1) F. Xu, L. Zhang, B. Cheng, J. Yu. Direct Z-Scheme TiO_2/NiS Core–Shell Hybrid Nanofibers with Enhanced Photocatalytic H_2-Production Activity. ACS Sustainable Chem. Eng. 2018, 6, 12291-12298.
2) A. Meng, B. Zhu, B. Zhong, L. Zhang, B. Cheng. Direct Z-scheme TiO_2/CdS hierarchical photocatalyst for enhanced photocatalytic H_2-production activity. Appl. Catal. B 2019, 243, 19-26.
3) J. Xiao, Y. Luo, Z. Yang, Y. Xiang, X. Zhang, H. Chen. Synergistic design for enhancing solar-to-hydrogen conversion over TiO_2 based ternary hybrid. Chen, Catal. Sci. Technol., 2018, 8, 2477-2487.
4) P. Jiménez-Calvo, V. Caps, M. Ghazzal, C. Colbeau-Justin, V. Keller. Au/TiO_2(P25)-gC_3N_4 composites with low g-C_3N_4 content enhance TiO_2 sensitization for remarkable H_2 production from water under visible-light irradiation. 2020, 75, 104888.
5) Y. Xiang, X. Wang, X. Zhang, H. Hou, K. Dai, Q. Huang, Hao Chen. Enhanced Visible Light Photocatalytic Activity of TiO_2 Assisted by Organic Semiconductor: A Structure Optimization Strategy of Conjugated Polymer. J. Mater. Chem. A, 2018, 6,153-159.
6) H. Hou, X. Zhang, D. Huang, X. Ding, S. Wang, X. Yang, S. Li, Y. Xiang, H. Chen. Conjugated microporous poly(benzothiadiazole)/TiO_2 heterojunction for visible-light-driven H_2 production and pollutant removal. Appl. Catal. B 2017, 203, 536-571.
7) T. Kuo, H. Liao, Y. Chen, C. Wei, C. Chang, Y. Chen, Y. Chang, J. Lin, Y. Lee, C. Wen, S. Li, K. Lin, D. Wang. Extended visible to near-infrared harvesting of earth-abundant FeS_2-TiO_2 heterostructures for highly active photocatalytic hydrogen evolution. Green Chem., 2018,20, 1640-1647.
8) X. Wei, C. Shao, X. Li, N. Lu, K. Wang, Z. Zhang, Y. Liu. Facile in situ synthesis of plasmonic nanoparticles-decorated g-C_3N_4/TiO_2 heterojunction nanofibers and comparison study of their photosynergistic effects for efficient photocatalytic H_2 evolution. Nanoscale, 2016,8, 11034-11043.
9) N. Guo, Y. Zeng, H. Li, X. Xu, H. Yu, X. Han. Novel mesoporous TiO2@g-C_3N_4 hollow core@shell heterojunction with enhanced photocatalytic activity for water treatment and H $_2$ production under simulated sunlight. J Hazard Mater. 2018, 353, 80-88.

10) D. Cao, Q. Wang, S. Zhu, X. Zhang, Y. Li, Y. Cui, Z. Xue, S, Gao. Hydrothermal construction of flower-like MoS_2 on TiO_2 NTs for highly efficient environmental remediation and photocatalytic hydrogen evolution. Sep. Purif. Technol, 2021, 265, 118463.
11) C. Gao, T. Wei, Y. Zhang, X. Song, Y. Huan, H. Liu, M. Zhao, J. Yu, X. Chen. A Photoresponsive Rutile TiO_2 Heterojunction with Enhanced Electron-Hole Separation for High-Performance Hydrogen Evolution. Adv. Mater. 2019, 31, 1806596.

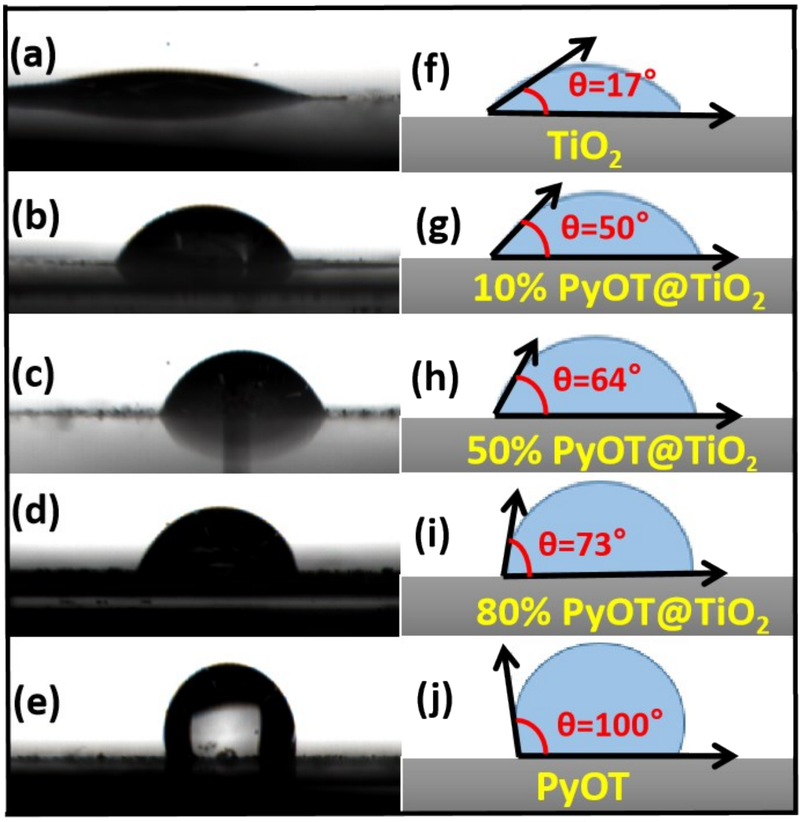

Fig. S10 Optical diagrams of H_2O droplets on samples TiO2 (a), 10% PyOT@TiO2 (b), 50% PyOT@TiO2 (c), 80% PyOT@TiO2 (d), and PyOT (e) surfaces, and their corresponding schematic interfaces and contact angles (f-j).

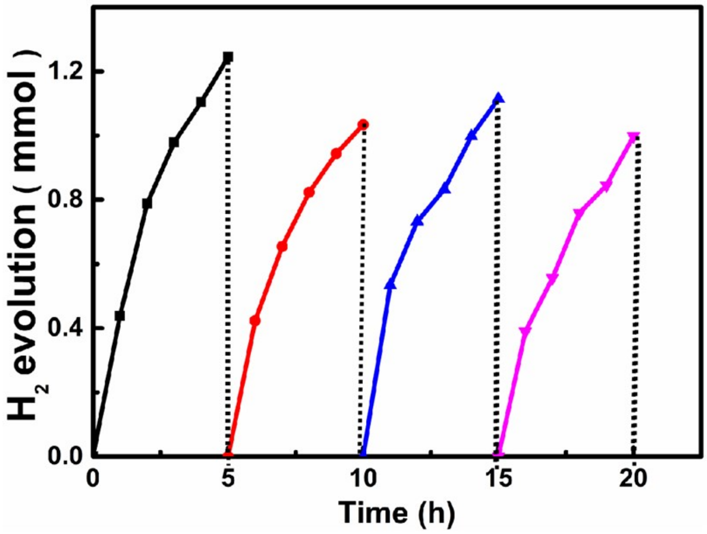

Fig. S11 Cycling test of H_2 evolution (evacuation every 5 h) for catalyst/H_2O/AA mixture (In the third run, AA was recharged).

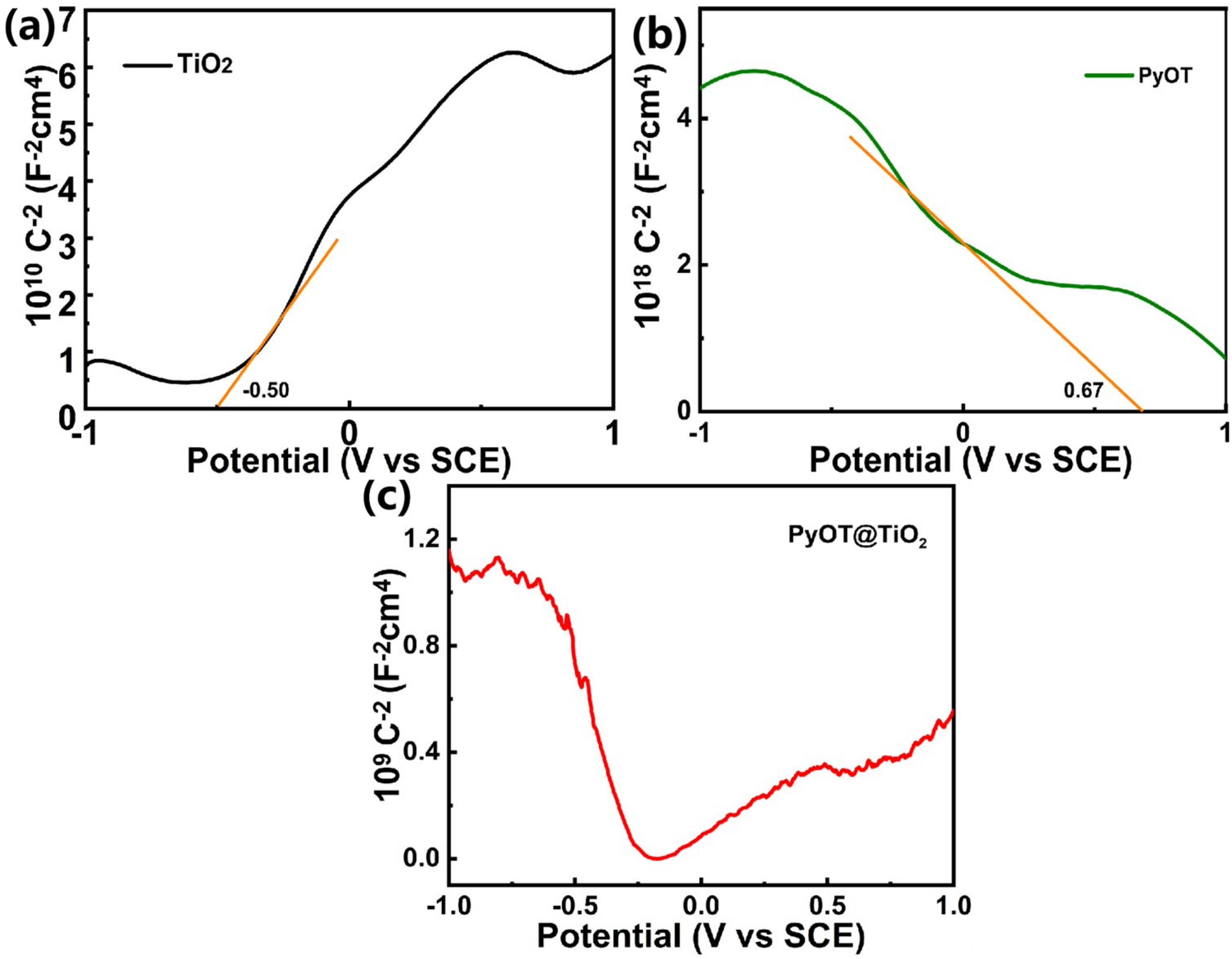

Fig. S12 Mott-Schottky (M-S) plots of TiO_2 (a) , PyOT(b), 50% PyOT@TiO_2 (c)**.**